British Journal of Pharmacology (2000) 130, 65–72
www.nature.com/bjp

Characterization of the binding of two novel glycine site antagonists to cloned NMDA receptors: evidence for two pharmacological classes of antagonists

[1]Bela Chopra, [1,2]Paul L. Chazot & *,[1]F. Anne Stephenson

[1]Department of Pharmaceutical and Biological Chemistry, School of Pharmacy, 29/39 Brunswick Square, London WC1N 1AX

1 The potency of two novel glycine site antagonists, GV150,526A and GV196,771A, was assessed by their ability to inhibit the binding of [^{3}H]-MDL105,519 to cell homogenates prepared from mammalian cells transfected with either NR1-1a, NR1-2a, NR1-1a/NR2A, NR1-1a/NR2B, NR1-1a/NR2C or NR1-1a/NR2D NMDA receptor clones.

2 The inhibition constants (K_is) for GV150,526A displacement of [^{3}H]-MDL105,519 binding to either NR1-1a or NR1-2a expressed alone were not significantly different and were best fit by a one-site binding model. GV150,526A inhibition to NR1-1a/NR2 combinations was best fit by a two-site model with the NR1-1a/NR2C having an approximate 2–4 fold lower affinity compared to other NR1-1a/NR2 receptors.

3 The K_is for GV196,771A displacement of [^{3}H]-MDL105,519 binding to NR1-1a, NR1-2a and all NR1-1a/NR2 combinations was best fit by a two-site binding model. There was no significant difference between the K_is for the binding to NR1-1a and NR1-2a; NR1-1a/NR2A receptors had an approximate 4 fold lower affinity for GV196,771A compared to other NR1-1a/NR2 combinations.

4 The K_is for both GV150,526A and GV196,771A for the inhibition of [^{3}H]-MDL105,519 binding to membranes prepared from adult rat forebrain were determined and compared to the values obtained for binding to cloned NMDA receptors.

5 The K_is for a series of glycine site ligands with diverse chemical structures were also determined for the inhibition of [^{3}H]-MDL105,519 binding to NR1-1a/NR2A receptors. L689,560 displayed similar binding characteristics to GV150,526A.

6 It is suggested that glycine site antagonists may be divided into two classes based on their ability to distinguish between NR1 and NR1/NR2 receptors with respect to binding curve characteristics. *British Journal of Pharmacology* (2000) **130,** 65–72

Keywords: NMDA receptor; glycine site antagonists; strychnine-insensitive glycine sites; ionotropic glutamate receptors; radioligand binding; MDL105,519

Abbreviations: ACEA1021, 5-nitro-6,7-dichloro-1,,4-dihydro-2,3-quinoxalinedione; CGP 6154, (±)-*trans*-4-[2-(4-azidophenyl)-acetylamino]-5,7-dichloro-1,2,3,4-tetrahydro-quinoline-2-carboxylic acid; DKA, 5,7 dichlorokynurenic acid; DMSO, dimethylsulphoxide; GV150,526A, (3-[2-(phenylaminocarbonyl)ethyl]-4,6-dichloroindole-2-carboxylic acid sodium salt; GV196, 771A (E-4,6-dichloro-3-(2-oxo-1phenyl-pyrrolidin-3-ylidenemethyl)-1H-indole-2-carboxylic acid; HEK, human embryonic kidney; $K_{i/D}$ dissociation/inhibition constant; L689,560, *trans*-2-carboxy-5,7-dichloro-4-phenylaminocarbonyl amino-1,2,3,4-tetrahydroquinoline; L701,324, 7-chloro-4-hydroxy-3-(3-phenoxy)phenyl-2(H)-quinolone; MDL105,519, (*E*)-3-(2)-phenyl-2-carboxyethenyl)-4,6-dichloro-1-indole-2-carboxylic acid; MK8O1, (+)-5-methyl-10,11dihydro-dibenzo[a,d]ccyclohepten-5,10-imine; NMDA, *N*-methyl-D-aspartate; NR1, NR2 etc., NMDA receptor subunit 1,2

Introduction

The *N*-methyl-D-aspartate (NMDA) subclass of glutamate receptor is an ionotropic receptor with a high permeability for Ca^{2+} requiring the binding of both the agonist, L-glutamate, and the co-agonist, glycine, for channel activation. NMDA receptors play a crucial role in long term potentiation (Bliss & Collingridge, 1993) and nociception (reviewed in Dickenson 1990). They are also involved in the pathophysiology of many neurological disorders including epilepsy and hypoxic damage (reviewed in Meldrum & Garthwaite, 1990). NMDA receptor antagonists have potential therefore as drugs for the treatment of cerebral ischaemia and neurotrauma. However, glutamate and non-competitive NMDA receptor antagonists such as the channel blocker, (+)-5-methyl-10, 11 dihydro-dibenzo[a,d]c-cyclohepten-5,10-imine (dizocilpine, MK801), have a plethora of side effects which include psychomimetic effects, memory impairment, neurotoxicity, tachycardia, and hypertension (reviewed in Danysz & Parsons, 1998). In contrast, glycine site antagonists with nanomolar affinity for the strychnine-insensitive glycine binding site of the NMDA receptor have been developed which have more promising therapeutic profiles. These include 5,7-dichlorokynurenic acid (DKA), L689,560 (*trans*-2-carboxy-5,7-dichloro-4-phenylaminocarbonyl amino-1,2,3,4-tetrahydroquinoline) and ACEA1021 (5-nitro-6,7-dichloro-1,4-dihydro-2,3-quinoxalinedione; reviewed in Danysz & Parsons, 1998). These compounds have served as templates for a new generation of glycine site antagonists which include substituted indole-2-carboxylates such as GV150,526A (3-[2-(phenylaminocarbonyl)ethyl]-4,6-dichlor-oindole-2-carboxylic acid sodium salt) and GV196,771A (E-4,6-dichloro-3-(2-oxo-1phenyl-pyrrolidin-3-ylidenemethyl)-1H-indole-2-carboxylic acid sodium salt). GV150,526A re-

*Author for correspondence; E-mail: fas@ulsop.ac.uk
[2]Current address: School of Health Sciences, University of Sunderland, Tyne and Wear, SR2 3SD, U.K.

duces the infarct area and protects against somatosensory evoked potentials in the middle cerebral occlusion model of focal ischaemia in the rat (Bordi *et al*., 1997). Furthermore it is devoid of amnestic side effects at doses well above the neuroprotective range of action (Bordi *et al*., 1997). It is currently in phase III clinical trials for treatment of stroke. GV196,771A's *in vivo* properties include a reduction in the pain sensitivity in the second phase of inflammation in the formalin test and it blocks the sensitization caused after chronic constriction injury of the left sciatic nerve in rat (Quartaroli *et al*., 1999). It has been suggested that GV196,771A is an anti-hyperalgesic compound useful in the treatment and prevention of chronic pain. GV150,526A and GV196,771A displace strychnine-insensitive [^{3}H]-glycine binding to membranes prepared from adult rat cerebral cortex with inhibition constants, $K_i = 3.2$ nM (Mugnaini *et al*., 1997) and $K_i = 28$ nM (Quartaroli *et al*., 1999) respectively.

The NMDA receptor is a hetero-oligomeric protein complex. There are six known NMDA receptor genes encoding three types of subunit, NR1, NR2 and NR3A. The NR1 subunit has eight distinct forms generated by alternative splicing designated NR1a,1b – NR4a,4b. Four separate genes encode the homologous NR2A – NR2D subunits. Functional NMDA receptors are assembled from a combination of both NR1 and NR2 subunits yielding receptor subtypes with distinct electrophysiological and pharmacological properties (reviewed in Hollmann & Heinemann, 1994; Sucher *et al*., 1996; Das *et al*., 1998). Site-directed mutagenesis, glycine site agonist and antagonist radioligand binding to cloned receptors as well as [^{3}H]-CGP 6154 ((±)-*trans*-4- [2-(4-azidophenyl)-acetylamino]-5, 7-dichloro-1,2,3,4-tetrahydro-quinoline-2-carboxylic acid) photoaffinity labelling has led to the localization of both agonist and antagonist glycine binding sites to the NR1 subunit (Hirai *et al*., 1996; Grimwood *et al*., 1995; Honer *et al*., 1998). The glutamate binding domain is formed by the NR2 subunits (Laube *et al*., 1997).

Here, we investigate the NMDA receptor subtype selectivity of GV150,526A and GV196,771A by assaying their ability to inhibit the binding of the glycine site antagonist, [^{3}H]-MDL105, 519 ((*E*)-3-(2)-phenyl-2-carboxyethenyl) -4,6-dichloro-1 [^{3}H]-indole-2-carboxylic acid), to both native and cloned NMDA receptors. Some of these results have been published in abstract form (Chopra *et al*., 1998; 1999).

Methods

Plasmid construction and transfection of cells

The full-length cDNAs encoding the rat NR1-1a, NR1-2a and mouse NR2A, NR2B and NR2C (alternative nomenclature NRϵ1, NRϵ2, NRϵ3) were subcloned into the mammalian expression vector pCIS, as previously described (Chazot *et al*., 1992; 1994; Cik *et al*., 1993). The cDNA encoding the mouse NR2D (alternative nomenclature NRϵ4), was excised from the pSPGR4 vector (Moriyoshi *et al*., 1991) and directionally cloned into the *Hind*III/*Eco*RI cloning sites of the pcDNA mammalian expression vector. Human embryonic kidney (HEK) 293 cells were cultured and transfected with NMDA receptor clones using the calcium phosphate precipitation method (Cik *et al*., 1993). HEK 293 cells were transfected with either each individual plasmid (10 μg total DNA) or pCISNR1-1a/pCISNR2A, pCISNR1-1a/pCISNR2B, pCISNR1-1a/pCISNR2C, pCISNR1-1a/pcDNANR2D binary combinations (10 μg total DNA in 1 : 3 ratios respectively). Cells transfected with pCISNR1-1a/pCISNR2A and pCISNR1-1a/pCISNR2B were grown in the presence of 1 mM ketamine post-transfection to prevent NMDA receptor-mediated cytotoxicity.

Preparation of P2 membranes and cell homogenates from HEK 293 transfected cells

Well-washed P2 membranes were prepared from adult Wistar rat forebrains as previously described (Chazot *et al*., 1993). Transfected HEK 293 cells were harvested 24 h post-transfection. The cell suspensions were centrifuged at $3000 \times g$ for 5 min at 4°C, the pellets collected and homogenized with a Dounce glass/glass homogenizer in ice-cold 50 mM Tris-citrate, pH 7.4, containing 5 mM EDTA, and 5 mM EGTA. The homogenate was recentrifuged at $30{,}000 \times g$ for 30 min at 4°C. The pellet was again homogenized and centrifuged. The final cell pellet was then resuspended in 50 mM Tris-citrate, pH 7.4, containing 5 mM EDTA, and 5 mM EGTA and either assayed immediately for [^{3}H]-MDL105,519 radioligand binding activity or analysed for the expression of the NMDA receptor subunits by immunoblotting using the appropriate anti-NMDA receptor subunit-specific antibodies (Chazot & Stephenson, 1997a,b).

Protein determination

Protein concentrations were determined by the method of Lowry *et al*. (1951) employing bovine serum albumin as the standard protein.

Radioligand binding assays

[^{3}H]-MDL105,519 competition radioligand binding assays were carried out by a rapid filtration assay (Chazot *et al*., 1998). Well-washed HEK 293 cells homogenates (50 – 100 μg protein) or adult rat P2 membranes (100 μg protein) in 50 mM Tris-citrate, pH 7.4, containing 5 mM EDTA, and 5 mM EGTA were incubated with [^{3}H]-MDL105,519 (1 nM) with either buffer or displacing drug to a final volume of 200 μl for 90 min at 4°C. Bound ligand was collected by rapid filtration using a Brandel cell harvester onto glass fibre filters (GF/B) which had been presoaked, in 50 mM potassium dihydrogen phosphate, pH 7.4 for at least 30 min at 4°C. The filters were washed rapidly three times with ice-cold 50 mM potassium dihydrogen phosphate, pH 7.4 (3×3 ml). Radioactivity was quantified using optiphase scintillation fluid (4 ml) by liquid scintillation spectroscopy. Non-specific binding was defined using 1 mM glycine in 50 mM Tris-citrate, pH 7.4. Stock solutions of GV150,526A and GV196,771A were dissolved in 10 mM KOH and 1% (v v^{-1}) dimethylsulphoxide (DMSO) respectively with subsequent dilutions for both into 50 mM Tris-citrate, pH 7.4. All other displacing drugs studied were dissolved in 0.1% (v v^{-1}) DMSO with subsequent dilution into 50 mM Tris-citrate, pH 7.4. [^{3}H]-MDL105,519 radioligand displacement binding assays using both GV150,526A and GV196,771A were carried out using borosilicate glass tubes. All other competition binding experiments were carried out in polypropylene tubes. Note that the inclusion of 10 mM KOH, and 0.1% (v v^{-1}) DMSO had no effect on [^{3}H]-MDL105,519 specific binding.

Data analysis

Results from the radioligand binding studies were analysed using non-linear least squares regression analysis using Graph PAD prism for both a one-site and a two-site binding model.

The *F*-test was used to assess whether the one-site or the two-site competition model best fit the data ($P<0.05$). The IC_{50} values for competition curves fitted to a one-site model were calculated from the following equation $Y=A+(B-A)/1+10^{X-\log IC_{50}}$ where A and B are the minimum and maximum percentage specific binding respectively, Y is the specific binding at a fixed concentration of displacing drug and $X=\log_{10}$ concentration of displacing drug. The IC_{50} values for competition curves fitted to a two-site competition model were calculated from $Y=A+(B-A)/(\text{Fraction } 1/1+10^{X-\log IC_{50(1)}})+(1-\text{Fraction}1/1+10^{X-\log IC_{50(2)}})$ where A, B, X and Y are the same as above: (1) and (2) are the high and low affinity sites. For the one-site and two-site binding models, the apparent inhibition constants (K_i) were calculated using the Cheng-Prusoff equation (Cheng & Prusoff, 1973), $K_i=IC_{50}/[1+(L/K_D)]$, where IC_{50} is the concentration of ligand giving 50% inhibition of specific binding, [L] is the [^{3}H]-MDL105,519 concentration and K_D = the dissociation constant for the binding of [^{3}H]-MDL105,519 to the appropriate NR1 or NR1-1a/NR2 combination (Chazot *et al*., 1998).

Materials

The expression vector pcDNA was obtained from Invitrogen (Netherlands). Ketamine was from Research Biochemicals Inc. (Natick, MA; U.S.A.). [^{3}H]-MDL105,519 (85 Ci mmol^{-1}) was purchased from Amersham International (Aylesbury, Bucks., U.K.). GV150,526A and GV196771A, (both > 99% purity as determined by both mass spectrometry and high performance liquid chromatography) were gifts from GlaxoWellcome (Verona, Italy). All other drugs were purchased from Tocris Neuramin (Bristol, U.K.). NMDA receptor cDNAs were generous gifts from Professors S. Nakanishi (Kyoto, Japan) and M. Mishina (Nigata, Japan). Human embryonic kidney 293 cells were a gift from Professor T. G. Smart (School of Pharmacy, London, U.K.), and the pCIS plasmid was a gift from Dr C. Gorman (Genentech, South San Francisco, CA, U.S.A.). All other materials were of the highest commercial purity available.

Results

Displacement of [^{3}H]-MDL105,519 binding to NR1 subunits expressed in HEK 293 cells by GV150,526A, GV196,771A and MDL105,519

We previously showed that [^{3}H]-MDL105,519 bound to both the NR1-1a and NR1-2a splice forms when each was expressed alone in HEK 293 cells with the same high affinity, i.e. $K_D \sim 3$ nM (Chazot *et al*., 1998). These two splice forms differ in that NR1-2a does not contain exon 21, a 37 amino acid insert also termed the C1 splice cassette which is found in NR1-1a adjacent to the transmembrane domain 4 in the intracellular C-terminal tail. Thus these two splice forms were also used for the characterization of the binding properties of GV150,526A and GV196,771A to NR1subunits expressed alone in mammalian cells. Further, since it was again previously shown that MDL105,519 did not distinguish between NR1-1a and NR1-2a with respect to binding affinity, displacement assays using MDL105,519 were always carried out in parallel with those for GV150,526A and GV196,771A. Competition binding between [^{3}H]-MDL105,519 and GV150,526A, MDL105,519 to both NR1-1a and NR1-2a was best fit to a one-site model (unpaired students *t*-test, $P<0.05$). Hill coefficients were close to unity and there was no significant difference in K_is between the different splice forms. The K_i values were for MDL105,519, 13 ± 5 nM (NR1-1a) and 11 ± 6 nM (NR1-2a) and for GV150,526A, 3.4 ± 1.5 nM (NR1-1a) and 5.0 ± 3.0 nM (NR1-2a). In contrast, GV196,771A binding to each of the NR1 splice variants was best fit by a two-site model (unpaired students *t*-test, $P<0.05$) with Hill coefficients significantly < 1, i.e. 0.6 ± 0.1, indicating the presence of more than one binding site. The high and low K_i values were respectively 8 ± 3 nM; 153 ± 41 nM (NR1-1a) and 4 ± 2 nM; 121 ± 20 nM (NR1-2a). The percentage contributions for the high and low affinity sites were $47\pm2\%$, $53\pm1\%$ (NR1-1a) and $48\pm2\%$, $52\pm2\%$ (NR1-2a). Figure 1 shows typical inhibition curves. The values are the means ± s.d. for $n=5$ binding curves from five separate transfections.

Displacement of [^{3}H]-MDL105,519 binding to binary NR1/NR2 subunit combinations by GV150,526A, GV196,771A, and MDL105,519

For all [^{3}H]-MDL105,519 binding studies to NR1/NR2 receptors expressed in HEK 293 cells, the expression of the respective NR2 subunit was always verified by immunoblotting using the appropriate anti-NR2 subunit antibody (results not shown). Also, as for the NR1 binding experiments, MDL105,519 displacement assays were always carried out in parallel with those for GV150,526A and GV196,771A. Displacement of [^{3}H]-MDL105,519 binding to all four NR1/NR2 combinations, i.e., NR1-1a/NR2A, NR1-1a/NR2B, NR1-1a/NR2C, and NR1-1a/NR2D recombinant receptors by both GV150,526A, and GV196,771A resulted in 100% inhibition curves which were best fitted to a two-site model (students *t*-test, $P<0.05$) with Hill coefficients in the range $0.4-0.6\pm0.2$. In contrast, the competition profile of MDL105,519 was significantly best fitted to a one-site model (students *t*-test, $P<0.05$) with Hill coefficients in the range $0.9-1.0\pm0.1$. Typical displacement curves for all three drugs using 1 nM [^{3}H]-MDL105,519 are shown in Figure 2, and Table 1 summarizes the apparent inhibition constants. These are the mean ± s.d. for $n=5$ displacement binding curves from $n=5$ transfections for each drug. There was no significant difference in the affinity of MDL105,519 for the heteromeric NMDA receptor subtypes investigated. The two sites that were resolved from the displacement of [^{3}H]-MDL105,519 binding to these heteromeric receptors by GV150,526A, and GV196,771A were present in approximately equal proportions; GV150,526A had an approximate 3 fold lower affinity for the NR1-1a/NR2C high affinity site whereas GV196,771A had an approximately 2 fold lower affinity for the NR1-1a/NR2A low affinity site.

Displacement of [^{3}H]-MDL105,519 binding to adult rat forebrain membranes by GV150,526A, GV196,771A, and MDL105,519

[^{3}H]-MDL105,519 competition curves were also carried out to membranes prepared from adult rat forebrain using GV150,526A, GV196,771A and MDL105,519. As before, MDL105,519 displacement assays were carried out in parallel with either GV150,526A or GV196,771A. Typical displacement curves are shown in Figure 3 and the K_is are summarized in Table 1. Both GV150,526A, and GV196,771A were best fitted to a two-site model whereas the competition profile for MDL105,519 was best fitted to a one-site sigmoidal model (students *t*-test, $P<0.05$). The Hill coefficients were 1.0 ± 0.1 (MDL105,519); 0.5 ± 0.1 (GV150,526A and GV196,771A). Within experimental error, MDL105,519 had the same K_i as

all four NR1/NR2 combinations; the binding affinities of GV150,526A and GV196,771A resembled most closely, heteromeric NR1-1a/NR2A, and NR1-1a/NR2B subunit combinations. As found for the heteromeric recombinant

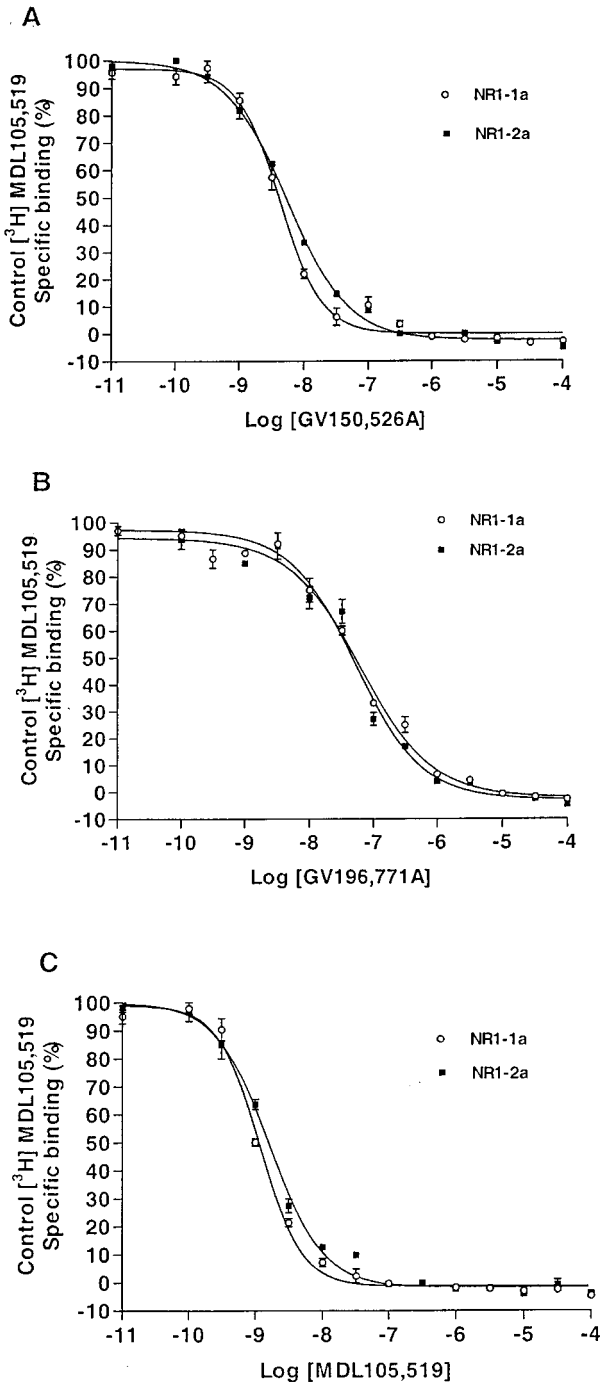

Figure 1 Competition profiles for the inhibition of [^{3}H]-MDL105,519 binding to NR1-1a and NR1-2a NMDA receptor subunits by GV150,526A, GV196,771A and MDL105,519. HEK293 cells were transfected with pCISNR1-1a or pCISNR1-2a (10 μg DNA), by the calcium phosphate method, cells were harvested 24 h post-transfection, well-washed cell homogenates prepared and [^{3}H]-MDL105,519 radioligand binding competition assays carried out all as described in Methods. (A) Displacement by GV150,526A; (B) Displacement by GV196,771A and (C), Displacement by MDL105,519. Data points are means$\pm$s.d. for five separate experiments from five independent transfections. MDL105,519, and GV150,526A inhibition of [^{3}H]-MDL105,519 binding to both of the NR1 splice forms was best fitted to one-site model. In contrast, GV196,771A binding to each of the NR1 splice variants was best fitted by a two-site model (unpaired students t-test, $P<0.05$).

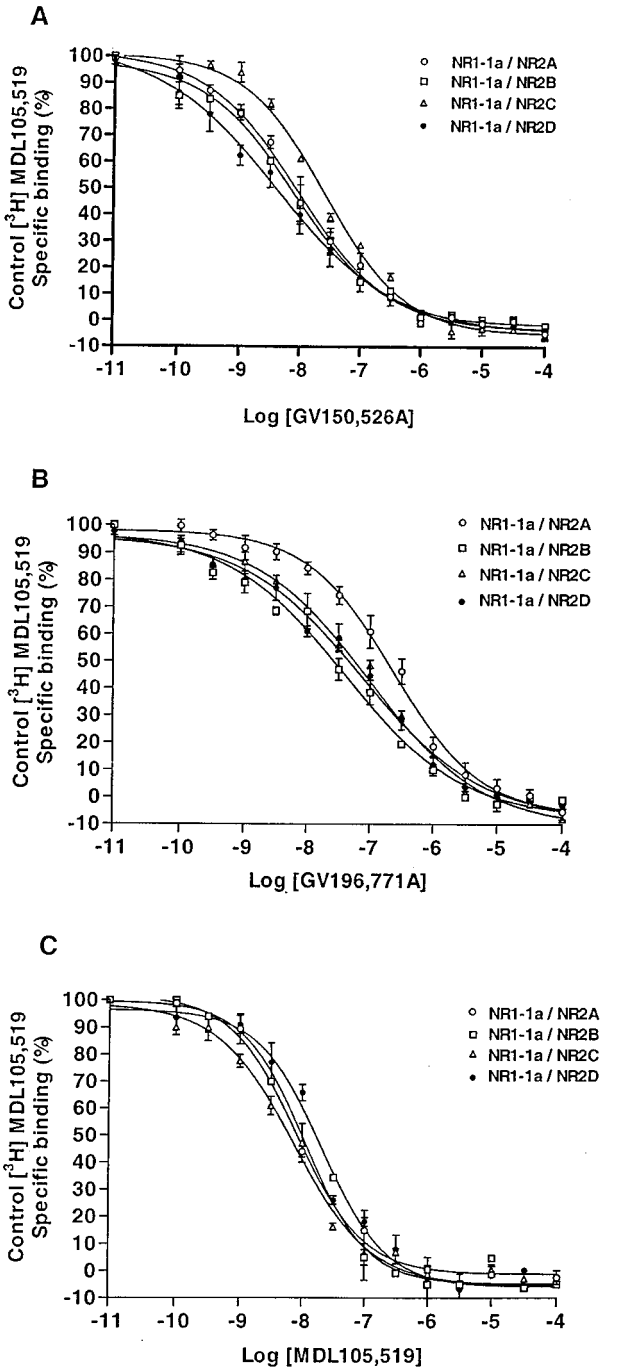

Figure 2 Competition curves for the inhibition of [^{3}H]-MDL105,519 binding by GV150,526A, GV196,771A and MDL105,519 to NR1-1a/NR2A, NR1-1a/NR2B, NR1-1a/NR2C and NR1-1a/NR2D cloned NMDA receptors. HEK293 cells were transfected with either pCISNR1-1a/pCISNR2A, pCISNR1-1a/pCISNR2B, pCISNR1-1a/pCISNR2C or pCISNR1-1a/pcDNANR2D (10 μg of DNA in a 1 : 3 ratio for NR1-1a : NR2 respectively) by the calcium phosphate precipitation method. Cells were harvested 24 h post-transfection, well-washed cell homogenates prepared and [^{3}H]-MDL105,519 radioligand binding competition assays carried out all as described in Methods. (A) Displacement by GV150,526A; (B) Displacement by GV196,771A; and (C) Displacement by MDL105,519. Data points are means$\pm$s.d. for five separate experiments from five independent transfections. MDL105,519 inhibition of [^{3}H]-MDL105,519 binding to all the heteromeric subtypes was best fit to a one-site model whereas both GV150,526A and GV196771A displaced binding to heteromeric receptors, which was best fit by a two-site model (unpaired students t-test, $P<0.05$). The apparent K_is are summarized in Table 1.

Table 1 A summary of the apparent K_is for GV150,526A, GV196,771A and MDL105,519 binding to cloned NR1/NR2 binary NMDA receptors expressed in HEK 293 cells

Receptor	*GV150,526A* K_i (nM)	*GV196,771A* K_i (nM)	*MDL105,519* K_i (nM)
NR1-1a/NR2A	0.7±0.2 (53±2)*	6±3 (37±6)*	12±4
	84±54 (47±2)*	484±260 (62±6)*	
NR1-1a/NR2B	0.5±0.1 (56±2)*	4±2 (55±4)*	15±5
	80±54 (44±2)*	220±100 (45±5)*	
NR1-1a/NR2C	3±1 (56±2)*	5.1±1 (55±4)*	12±6
	109±47 (44±2)*	180±20 (45±5)*	
NR1-1a/NR2D	0.4±0.1 (56±2)*	4±2 (55±4)*	18±7
	47±25 (44±2)*	153±70 (45±5)*	
Adult rat forebrain	2.6±1.2 (51±3)*	9.2±7.2 (44±5)*	15±10
	42±34 (49±3)*	400±150 (56±6)*	

MDL105,519 inhibition of [^{3}H]-MDL 105,519 binding to all four binary NMDA receptor combinations was best fitted to a one-site model. GV150,526A and GV196,771A inhibition of [^{3}H]-MDL 105,519 binding to all four combinations was best fitted to a two-site model (unpaired student's *t*-test, $P<0.05$). *Values are the apparent K_is for the two-site binding model with the percentage contribution for each site given in brackets.

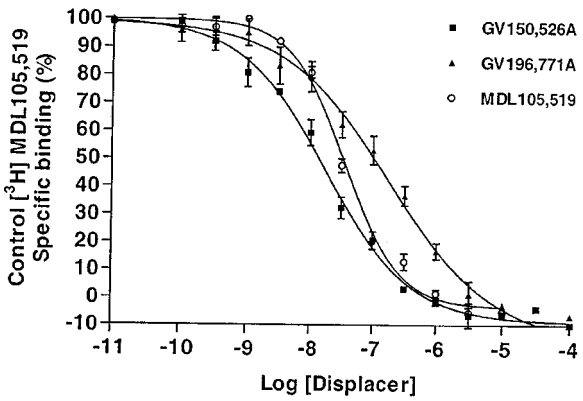

Figure 3 Competition curves for the inhibition of [^{3}H]-MDL105,519 binding by GV150,526A and GV196,771A to membranes prepared from adult rat forebrain. Membranes were prepared from adult rat forebrains and [^{3}H]-MDL105,519 radioligand binding competition assays carried out as described in Methods for GV150,526A, GV196,771A and MDL105,519. Data points are means±s.d. for three separate experiments. The apparent inhibitory constants (K_is) are summarized in Table 1.

receptors, the abundance of the binding sites resolved by the two-site model was approximately 50%.

Displacement of [^{3}H]-MDL105,519 binding to NR1-1a/NR2A receptors expressed in HEK 293 cells by glycine, DKA, L701,324, and L689,560

Competition profiles for the inhibition of [^{3}H]-MDL105,519 binding to NR1-1a/NR2A receptors by other glycine site ligands with diverse chemical structures were carried out to establish whether these could also resolve more than one binding site as found for the displacement of [^{3}H]-MDL105,519 binding to NR1/NR2 receptors by GV150,526A, and GV196,771A. Figure 4 shows the resultant competition curves for the inhibition of [^{3}H]-MDL105,519 binding to NR1-1a/NR2A receptors by glycine, DKA, L701,324 (7-chloro-4-hydroxy-3-(3-phenoxy)phenyl-2(H)-quinolone), and L689,560. Hill coefficients were close to unity for glycine, DKA and L701,324 displacement curves. Values were, 1.0±0.1; 0.9±0.2 and 1.0±0.1 respectively. The displacement curve for L689,560 however, was best fitted by a two-site model with a

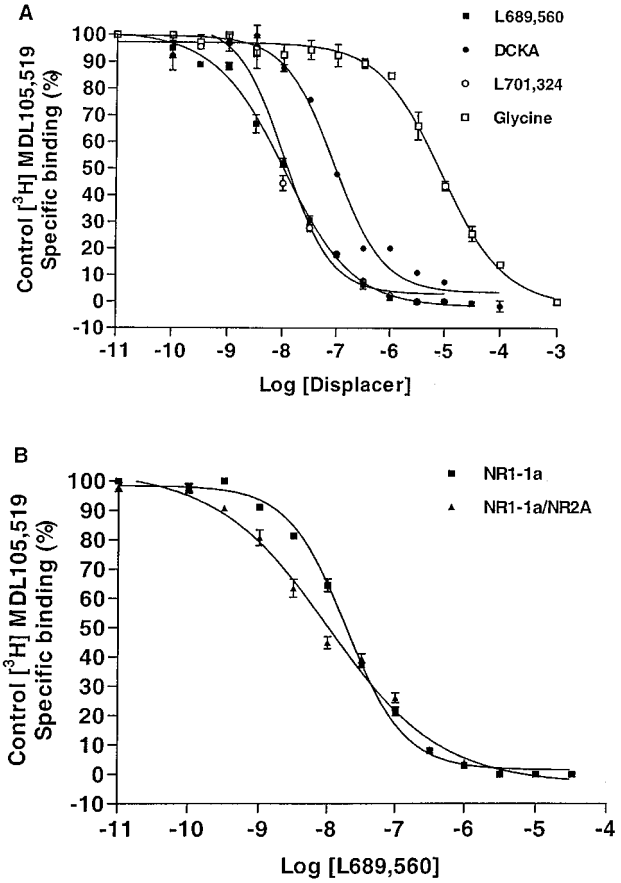

Figure 4 Competition curves for the inhibition of [^{3}H]-MDL105,519 binding to NR1-1a/NR2A receptors expressed in HEK 293 cells by glycine, DKA, L701,324 and L689,560. HEK 293 cells were transfected with either pCISNR1-1a/pCISNR2A (A, 10 μg of DNA in a 1:3 ratio) or pCISNR1-1a (B) by the calcium phosphate precipitation method. Cells were harvested 24 h post-transfection, well-washed cell homogenates prepared and [^{3}H]-MDL105,519 radioligand binding competition assays carried out all as described in Methods. Data points are means±s.d. for three separate experiments from three independent transfections. For (A) glycine, DKA and L701,324 inhibition of [^{3}H]-MDL105,519 binding was best fit to a one-site model whereas L689,560 was best fit by a two-site compared to a one-site model (unpaired students *t*-test, $P<0.05$). (B) L689,560 inhibition of [^{3}H]-MDL105,519 binding was best fitted by a two-site compared to a one-site model for NR1-1a/NR2A but by a one-site fit for NR1-1a (unpaired students *t*-test, $P<0.05$).

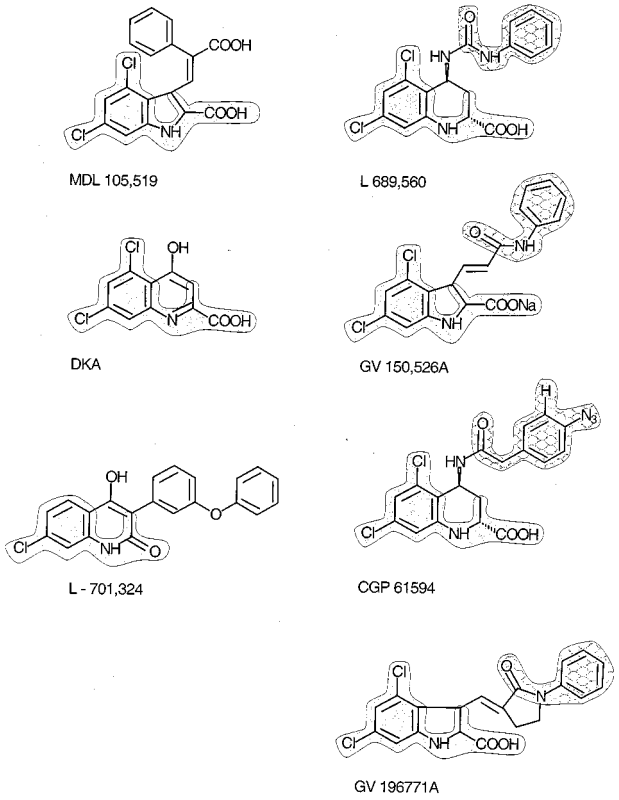

Figure 5 Chemical structures of glycine site ligands. The filled areas show the molecule determinants shared by all the glycine site antagonists; the hatched areas show the structural moieties shared between those antagonists which display complex binding behaviour in [^{3}H]-MDL105,519 inhibition assays.

Hill coefficient significantly less than one, 0.6 ± 0.2 (unpaired students *t*-test, $P < 0.05$). K_i values were:- glycine, 3900 ± 1000 nM; DKA, 50 ± 10 nM; L701,324, 4.2 ± 1.1 nM and L689,560, 2.4 ± 0.7 nM and 70 ± 43 nM, with 46 ± 4% and 54 ± 4% percentage contributions to each site respectively. Note that the displacement curve for the inhibition of [^{3}H]-MDL105,519 binding to NR1-1a by L689,560 was best fitted by a one-site binding model (Figure 4).

Discussion

In this study, the binding properties of two glycine site antagonists, GV150,526A and GV196,771A, to both native and cloned NMDA receptor subtypes expressed transiently in HEK 293 cells were characterized using the glycine site antagonist radioligand, [^{3}H]-MDL105,519. GV150,526A and GV196,771A both displaced [^{3}H]-MDL105,519 radioligand binding with high affinity from NR1-1a, NR1-2a and NR1-1a/NR2 receptors. Overall, GV196,771A had an approximate 10 fold lower affinity than GV150,526A for all NMDA receptor subtypes studied including those expressed in adult rat forebrain. These findings are in agreement with previous binding studies where it was shown that both GV150,526A and GV196,771A are high affinity ligands for the strychnine-insensitive glycine binding site of the NMDA receptor (Mugnaini *et al.* 1997; Quartaroli *et al.*, 1999), the major determinants for high affinity glycine site antagonists reside on the NR1 subunit and that the 37 amino acids of the C1 exon present in the NR1-1a but not the NR1-2a splice variant does not effect antagonist binding affinity (Siegel *et al.*, 1996; Grimwood *et al.*, 1995; Laurie & Seeburg, 1994; Chazot *et al.*, 1998). However, the interesting finding was that for GV150,526A in NR1-1a/NR2 combinations and in native brain membranes, the Hill coefficients of all four displacement curves were significantly < 1 and were best fitted by a two-site binding model. For GV196,771A, the situation was more complex since all displacement curves, i.e. binding to NR1-1a, NR1-2a, NR1-1a/NR2 or brain membranes yielded Hill coefficients < 1 and were best fitted by a two-site model.

Biphasic, concave inhibition curves may be the result of either impurity and/or stability of the displacing ligand; binding to a heterogeneous population of receptors which have different affinities for the ligand; the existence of two binding sites within a receptor with different affinities for the ligand; different states of an apparently single binding site and negative co-operativity. For GV150,526A, the biphasic binding curve is coincident with the presence of the NR2 subunit since displacement assays carried out in parallel and under identical conditions to NR1-1a and NR1-1a/NR2 yielded one-site and two-site fits respectively thus together with the > 99% purity determined by high performance liquid chromatography and mass spectrometry eliminates ligand impurity and stability as a possible explanation for heterogeneity.

When mammalian cells are transfected with NR1 and NR2 clones, the expressed receptors are heterogeneous being a mixture of unassembled NR1 and assembled NR1/NR2 complexes (Chazot & Stephenson, 1997b). The biphasic displacement curves may therefore be explained by GV150,526A having lower affinity for NR1/NR2 compared to NR1 receptors. The high affinity K_is for the two-site fit are in approximate agreement with the K_i values for binding to NR1-1a single subunits (*c.f.* Table 1 and Results). When the NR1-1a subunit is expressed alone, it has been reported that it does not reach the cell surface but it is retained in intracellular occlusions associated with the endoplasmic reticulum (McIlhinney *et al.*, 1998). Thus the one-site versus two-site models may be resolved by the displacement of [^{3}H]-MDL105,519 binding by GV150526A to cell surface receptors rather than to homogenates of transfected cells where putative intracellular pools are accessed by the hydrophilic radioligand. However, Ehlers *et al.* (1995) found that NR1 splice forms containing the first COOH-terminal cassette, C1, i.e. NR1-1a and NR1-3a, when expressed alone in fibroblast cells were located in discrete, receptor-rich domains associated with the plasma membrane in contrast to the splice variants lacking this cassette (NR-2a and NR-4a) which were distributed throughout the cell. The resolution of these studies did not permit distinction between NR1-1a labelling expressed on the cell surface or NR1-1a labelling localized to the intracellular face of the membrane. If NR1-1a is expressed at the cell surface, it would exclude the possibility of distinguishing between NR1-1a and NR1-1a/NR2A receptors by cell surface binding studies.

In a previous study, [^{3}H]-GV150,526A in the concentration range, 0.3 – 30 nM, and using glycine to measure the non-specific binding, bound with a single high affinity site to membranes prepared from rat brain (Mugnaini *et al.*, 1997). This is in contrast to the results reported here in that the displacement of [^{3}H]-MDL105,519 binding by GV150,526A to brain membranes was best fit by a two-site model. The discrepancies may be explained by the narrow range of [^{3}H]-GV150,526A used, i.e. 0.3 – 30 nM with the K_i (low affinity) for NR1/NR2A or NR1/NRB, the most prevalent receptor subtypes, being $K_i = 80$ nM and the inherent difficulty of using [^{3}H]-GV150,526A. The

latter results in low signal:noise ratios at high [^{3}H]-GV150,526A concentrations thus making deviation from one-site binding difficult to detect.

Several other glycine site antagonists were studied in [^{3}H]-MDL105,519 displacement assays to see if under the assay conditions used here, they exhibited similar behaviour to GV150,526A. Of the five compounds, only L689,560 yielded a one-site fitted to NR1-1a and a two-site fit to NR1-1a/NR2A receptors. Grimwood *et al*. (1995) also reported a Hill coefficient of 1.00 for the displacement of [^{3}H]-L689,560 binding by unlabelled L689,560 to both singly expressed NR1-1a and NR1-4a subunits. No binding information has yet been published for NR1/NR2 combinations. However, displacement by L689,560 in either [^{3}H]-L689,560 or [^{3}H]-glycine inhibition assays to rat brain also yielded a Hill coefficient of 1.0 although the rates of dissociation/association were both better fitted by a double exponential suggestive of heterogeneity of sites (Grimwood *et al*., 1992). In another study, Parsons *et al*. (1997) found that L689,560 displaced the binding of [^{3}H]-MDL105,519 to rat cerebral cortical membranes with a Hill coefficient = 1.13.

Although to our knowledge, this is the first time that glycine site antagonist binding has been found to be best fitted by a two-site binding model and that this property has been ascribed to the NR2 subunit even though the major determinants for high affinity binding are localized within the NR1 subunit, there is some evidence which suggests that NR2 subunits may contribute to the affinity of this site. For example, MDL105,519 does not distinguish between all four NR1-1a/NR2 forms but in functional studies, L689,560 has a 5 fold selectivity for NR1-1a/NR2A compared to NR1-1a/NR2B receptors and notably, the antagonist response curve for NR1-1a/NR2A deviated from sigmoidal behaviour (Hess *et al*., 1996); DKA has an approximate 2 fold lower affinity for NR1-NR2B, NR1/NR2D compared to NR1/NR2A and NR1/NR2C (Laurie & Seeburg, 1994). More recently, it was shown that [^{3}H]-CGP 61594, a glycine site antagonist which is also a photoaffinity ligand, preferentially labelled NR2B-subunit containing NMDA receptors although the incorporated radioactivity was associated with only the $M_r \sim 120\,000$ NR1 subunit (Honer *et al*., 1998). A low affinity reversible binding site for [^{3}H]-CGP 61594 was found in rat cerebellar membranes. It was attributed to binding to NR1/NR2A, NR1/NR2C or both subtypes of receptor since these are the subunits expressed in adult cerebellum (Honer *et al*., 1998).

The displacement of [^{3}H]-MDL105,519 binding by GV196,771A was best fitted by a two-site model for both singly NR1-1a and doubly NR1-1a/NR2A transfected HEK 293 cells. Physiological and molecular biological studies are both consistent with there being two high affinity glycine binding sites per NMDA receptor oligomer. The bulky pyrrole group of GV196,771A may sterically hinder the binding of the second GV196,771A molecule resulting in negative co-operativity and a biphasic displacement curve. This may occur for both NR1-1a/NR2A and $(NR1\text{-}1a)_x$ receptors. Thus it is proposed that glycine site antagonists may be subdivided into two pharmacological classes, i.e. those that show simple, bimolecular competitive behaviour with regard to inhibition of [^{3}H]-MDL105,519 radioligand binding and those that result in complex inhibition curves. This may be due to the ability of the latter to distinguish between NMDA receptor subpopulations with regard to binding affinity. Figure 5 shows the structures of the glycine site antagonists used here. The figure highlights the parts of the molecules shared by all the antagonists. It is noticeable that the substituted indole-2-carboxylate antagonists which show complex binding behaviour are trans stereoisomers with six spacer bonds, all have substituted phenyl amide moieties and a secondary or tertiary amide (GV196 771A) as shown (Figure 5). Chemical differences between GV150,526A and GV196,771A include the secondary versus tertiary amide and the presence of the pyrrole group in GV196,771A which may contribute significant hydrophobic and/or steric interactions to the binding between receptor and ligand. However, more compounds will need to be screened/re-screened to address structure/function relationships in more detail in the context of NMDA receptor subtype-selectivity.

Bela Chopra holds a postgraduate PhD studentship funded by GlaxoWellcome, Verona, Italy. We thank GlaxoWellcome, Verona, Italy for GV150,526A and GV196,771A, Drs S. Nakanishi and M. Mishina for the generous gifts of NMDA receptor clones and Annie Cavanagh for Figure 5. We also acknowledge the contribution of Dr Lynda Hawkins in valuable discussions.

References

BLISS, T.V.P. & COLLINGRIDGE, G.L. (1983). A synaptic model of memory: long-term potentiation in the hippocampus. *Nature,* **361,** 31 – 39.

BORDI, F., PIETRA, C., ZIVIANI, L. & REGGIANI, A. (1997). The glycine site antagonist GV150526A protects somatosensory evoked potentials and reduces the infarct area in the MCAo model of focal ischaemia in the rat. *Exp. Neurol.,* **145,** 425 – 433.

CHAZOT, P.L., CIK, M. & STEPHENSON, F.A. (1992). Immunological detection of the NMDAR1 glutamate receptor subunit expressed in human embryonic kidney 293 cells and in rat brain. *J. Neurochem.,* **59,** 1176 – 1178.

CHAZOT, P.L. & STEPHENSON, F.A. (1997a). Molecular dissection of native mammalian forebrain NMDA receptors containing the NR1 C2 exon: Direct demonstration of NMDA receptors comprising NR1, NR2A, and NR2B subunits within the same complex. *J. Neurochem.,* **69,** 2138 – 2144.

CHAZOT, P.L. & STEPHENSON, F.A. (1997b). Biochemical evidence for the existence of a pool of unassembled C2 exon-containing NR1 subunits of the mammalian forebrain NMDA receptor. *J. Neurochem.,* **68,** 507 – 516.

CHAZOT, P.L., REISS, C., CHOPRA, B. & STEPHENSON, F.A. (1998). [^{3}H]MDL 105,519 binds with equal high affinity to both assembled and unassembled NR1 subunits of the NMDA receptor. *Eur. J. Pharmacol.,* **353,** 137 – 140.

CHAZOT, P.L., COLEMAN, S.K., CIK, M. & STEPHENSON, F.A. (1994). Molecular characterisation of *N*-methyl-D-aspartate receptor expressed in mammalian cells yields evidence for the coexistence of three subunit types within a discrete receptor molecule. *J. Biol. Chem.,* **39,** 24403 – 24409.

CHAZOT, P.L., FOTHERBY, A. & STEPHENSON, F.A. (1993). Evidence for the involvement of a carboxyl group in the vicinity of the MK801 and magnesium ion binding site of the *N*-methyl-D-aspartate receptor. *Biochem. Pharmacol.,* **45,** 605 – 610.

CHENG, Y.-C. & PRUSOFF, W.H. (1973). Relationship between the inhibition constant (K_i) and the concentration of inhibitor which causes 50 percent inhibition (IC_{50}) of an enzymatic reaction. *Biochem. Pharmacol.,* **22,** 3099 – 3108.

CHOPRA, B., CHAZOT, P.L., MUGNAINI, M. & STEPHENSON, F.A. (1998). An investigation into the NMDA receptor subtype selectivity of two novel glycine site antagonists. *Br. J. Pharmacol.,* **123,** (Suppl): 131P.

CHOPRA, B., CHAZOT, P.L., MUGNAINI, M. & STEPHENSON, F.A. (1999). A comparison between the binding affinities of two novel glycine site antagonists to cloned NMDA receptor subtypes. *Br. J. Pharmacol.,* **126,** (Suppl.): 254.

CIK, M., CHAZOT, P.L. & STEPHENSON, F.A. (1993). Optimal expression of cloned NMDAR1/NMDAR2A heteromeric glutamate receptors: A biochemical characterisation. *Biochem. J.,* **296,** 877 – 883.

DANYSZ, W. & PARSONS, C.G. (1998). Glycine and NMDA receptors: Physiological significance and possible therapeutic applications. *Pharmacol. Rev.,* **50,** 597 – 664.

DAS, S., SASAKI, Y.F., ROTHE, T., PREMKUMAR, L.S., TAKASU, M., CRANDALL, J.E., DIKKES, P., CONNER, D.A., RAYUDU, P.V., CHENG, W., CHEN, H.S.V., LIPTON, S.A. & NAKANISHI, N. (1998). Increased NMDA current and spine density in mice lacking the NMDA receptor subunit NR3A. *Nature,* **393,** 377 – 381.

DICKENSON, A.H. (1990). A cure for wind up: NMDA receptor antagonists as potential analgesics. *Trends Pharmacol. Sci.,* **11,** 307 – 309.

EHLERS, D.M., TINGLEY, G.W. & HUGANIR, R.L. (1995). Regulated subcellular distribution of the NR1 subunit of the NMDA receptor. *Science,* **269,** 1734 – 1737.

GRIMWOOD, S., BOURDELLES, B. & WHITING, P. (1995). Recombinant human NMDA homomeric NR1 receptors expressed in mammalian cells form a high affinity glycine binding site. *J. Neurochem.,* **64,** 525 – 530.

GRIMWOOD, S., MOSELEY, M.A., CARLING, W.R., LEESON, D.P. & FOSTER, C.A. (1992). Characterisation of the binding of L689,560, an antagonist for the glycine site on the *N*-methyl-D-aspartate receptor, to rat brain membranes. *Mol. Pharmacol.,* **41,** 923 – 930.

HESS, S.D., DAGGETT, L.P., CRONA, J., DEAL, C., LU, C.-C., URRUTIA, A., CHAVEZ-NORIEGA, L., ELLIS, S.B., JOHNSON, E.C. & VELICELEBI, G. (1996). Cloning and functional characterization of human heteromeric N-methyl-D-aspartate receptors. *J. Pharmacol. Exp. Ther.,* **278,** 808 – 816.

HIRAI, H., KIRSCH, J., LAUBE, B., BETZ., H. & KUHSE, J. (1996). The glycine binding site of the *N*-methyl-D-aspartate receptor subunit NR1: Identification of novel determinants of co-agonist potentiation in the extracellular M3-M4 loop region. *Proc. Natl. Acad. Sci. U.S.A.,* **93,** 6031 – 6036.

HOLLMANN, M. & HEINEMANN, S. (1994). Cloned glutamate receptors. *Ann. Rev. Neurosci.,* **17,** 31 – 108.

HONER, M., BENKE, D., LAUBE, B., KUHSE, J., HECKENDORN, H.A., ANGUST, C., MONYER, H., SEEBURG, P.H., BETZ, H. & MOHLER, H. (1998). Differentiation of glycine antagonist sites of *N*-methyl-D-aspartate receptor subtypes: Preferential interaction of CGP61594 with NR1/NR2B receptors. *J. Biol. Chem.,* **273,** 11158 – 11163.

LAUBE, B., HIRAI, H., STURGESS, M., BETZ, H. & KUHSE, J. (1997). Molecular determinants of agonist discrimination by NMDA receptor subunits: analysis of the glutamate binding site on the NR2B subunit. *Neuron,* **18,** 493 – 503.

LAURIE, D.J. & SEEBURG, P.H. (1994). Ligand affinities at recombinant *N*-methyl-D-aspartate receptor depend on subunit composition. *Eur. J. Pharmacol.,* **68,** 335 – 345.

LOWRY, O.H., ROSEBROUGH, N.J., FARR, A.L. & RANDALL, R.J. (1951). Protein measurement with the Folin phenol reagent. *J. Biol. Chem.,* **193,** 265 – 275.

MCILHINNEY, R.A.J., BOURDELLES, B.L., MOLNÁR, E., TRICAUD, N., STRIET, P. & WHITING, P.J. (1998). Assembly, intracellular targeting and cell surface expression of the human N-methyl-D-aspartate receptor subunits NR1 and NR2A in transfected cells. *Neuropharmacology,* **37,** 1355 – 1367.

MELDRUM, B. & GARTHWAITE, J. (1990). Excitatory amino acid neurotoxicity and neurodegenerative diseases. *Trends Pharmacol. Sci.,* **11,** 379 – 387.

MORIYOSHI, K., MASU, M., ISHII, T., SHIGEMOTO, R., MIZUNO, N. & NAKANISHI, S. (1991). Molecular cloning and characterization of the rat NMDA receptor. *Nature,* **354,** 31 – 37.

MUGNAINI, M., DAL FORNO, G., CORSI, M. & BUNNEMANN, B. (2000). Receptor binding characteristics of the novel NMDA receptor glycine site antagonist [^{3}H]GV150526A in rat cerebral cortical membranes. *Eur. J. Pharmacol., In press*

PARSONS, C.G., DANYSZ, W., QUACK, G., HARTMANN, S., LORENZ, B., WOLLENBURG, C., BARAN, L., PRZEGALINSKI, E., KOSTOWSKI, W., KRZAZCIK, P., CHIZH, B. & HEADLEY, P.M. (1997). Novel systemically active antagonists of the glycine site of the N-methyl-D-aspartate receptor: Electrophysiological, biochemical and behavioral characterisation. *J. Pharmacol. Exp. Ther.,* **283,** 1264 – 1275.

QUARTAROLI, M., CARIGNANI, C., DAL FORNO, G., MUGNAINI, M., UGOLINI, A., ARBAN, R., BETTELINI, L., MARAIA, G., BELARDETTI, F., REGGIANI, A., TRIST, D.G., RATTI, E., DI FABIO, R. & CORSI, M. (1999). Potent antihyperalgesic activity without tolerance produced by glycine site antagonist of N-methyl-D-asparate receptor GV196771A. *J. Pharmacol. Exp. Ther.,* **290,** 158 – 169.

SIEGEL, W.B., SREEKRISHNA, K. & BARON, M.B. (1996). Binding of the radiolabelled glycine site antagonist [^{3}H] MDL105,519 to homomeric NMDA-NR1a receptors. *Eur. J. Pharmacol.,* **312,** 357 – 365.

SUCHER, N.J., AWOBULUYI, M., CHOI, Y. & LIPTON, S.A. (1996). NMDA receptors: From genes to channels. *Trends Pharmacol. Sci.,* **17,** 348 – 355.

(Received November 9, 1999
Revised January 31, 2000
Accepted February 8, 2000)